NATIONAL ADVISORY COMMITTEE FOR AERONAUTICS

TECHNICAL NOTE 2583

A SEMIEMPIRICAL PROCEDURE FOR COMPUTING THE WATER-PRESSURE DISTRIBUTION ON FLAT AND V-BOTTOM PRISMATIC SURFACES DURING IMPACT OR PLANING

By Robert F. Smiley

Langley Aeronautical Laboratory
Langley Field, Va.

NACA

Washington
December 1951

1G

NATIONAL ADVISORY COMMITTEE FOR AERONAUTICS

TECHNICAL NOTE 2583

A SEMIEMPIRICAL PROCEDURE FOR COMPUTING THE WATER-PRESSURE DISTRIBUTION ON FLAT AND V-BOTTOM PRISMATIC SURFACES DURING IMPACT OR PLANING

By Robert F. Smiley

SUMMARY

A semiempirical procedure is presented for computing the water-pressure distribution on flat and V-bottom prismatic surfaces during planing or landings. For the rectangular flat plate, a consideration of several previous theoretical derivations and some observations of the experimental data lead to the development of simple equations which are in good agreement with experimental data for trims below 30° and for wetted-length-beam ratios at least up to 3.3. This development is based primarily on the assumption that the longitudinal distribution of pressure on a rectangular flat plate is substantially a function only of the normal-load coefficient so that this distribution may be computed from the existing theory for two-dimensional flow. The transverse distribution of pressure is obtained as a compromise between the available theoretical treatments for very small and very large wetted-length-beam ratios. For a V-bottom prismatic surface with appreciable chine immersion, the pressures on chine-immersed sections of a model having an angle of dead rise of 30° are found to be very similar to those on the corresponding flat plate so that a simple modification of the flat-plate equations can be used to predict approximately the pressures on V-bottom surfaces.

INTRODUCTION

In order to determine the magnitude and distribution of the water pressure on seaplanes during planing or landings, a large amount of theoretical and experimental research has been conducted, most of which has dealt with the problem of a V-bottom prismatic surface (including the case of the rectangular flat plate). Although neither the available theories nor the available experimental data are as yet adequate to predict accurately the pressure distribution on V-bottom surfaces

for arbitrary landing or planing conditions, a consideration of several of the available theories and some observations of experimental pressure-distribution data for a flat plate and a model having an angle of dead rise of 30° have been found to lead to a simple approximate semiempirical procedure for computing the pressure distribution. The purpose of this paper is to present this semiempirical procedure and to determine its value from comparisons of calculated and experimental pressure distributions.

The theoretical derivations used in this analysis are as follows: (1) the derivation of Wagner for the pressure distribution on a rectangular flat plate during steady planing for two-dimensional flow (references 1 to 3), (2) the derivation of Korvin-Kroukovsky and Chabrow for the pressure distribution on a submerged wedge having steady separated two-dimensional flow behind the wedge (reference 4), and (3) the derivation of Wagner for the pressure distribution on non-chine-immersed sections of a straight-side wedge during an impact for very small trims (references 1, 5, and 6) which has been modified by Pierson and Leshnover to apply to practical trims (references 6 and 7). Also used is the fact that the pressure distributions during planing and impact are very similar and can be correlated approximately according to the relations given in references 8 and 9.

In this paper a review of these theories is first made and the results and equations pertinent to this analysis are given. Some of the results of the theories are then synthesized to form the semiempirical procedure for computing the pressure distribution. This synthesis proceeds according to the following outline:

(1) The rectangular flat plate

- (a) General observations of the experimental data
- (b) Consideration of the transverse pressure distribution
- (c) Consideration of the longitudinal center-line pressure distribution
- (d) Proposed procedure for predicting the pressure distribution
- (e) Limitations of method

(2) The V-bottom surface

- (a) Consideration of the transverse pressure distribution on non-chine-immersed and chine-immersed sections
- (b) Consideration of the longitudinal center-line pressure distribution on chine-immersed sections
- (c) Proposed procedure for computing the pressure distribution

SYMBOLS

A	hydrodynamic aspect ratio
b	beam of model, feet
c	wetted semiwidth of model in any transverse section, feet
$\dot{f}$	equivalent planing velocity, feet per second $\left(\dot{f} = \dot{x} + \dot{y} \cot \tau = \frac{\dot{z}}{\sin \tau}\right)$
F_N	hydrodynamic force normal to keel (normal to surface for flat plate), pounds
h	theoretical constant $\left(\frac{\pi - 2\beta}{\pi}\right)$
k	theoretical constant defined following equation (7)
K	water-rise ratio
p	instantaneous pressure, pounds per square inch
$\overline{p}/p_c$	average value of p/p_c in any transverse section
$\dot{s}$	instantaneous velocity of model parallel to longitudinal center line of model, feet per second $(\dot{x} \cos \tau - \dot{y} \sin \tau)$
S	projection of wetted area normal to keel, square beams $\left(\lambda_p b^2$ for rectangular flat plate$\right)$
t	time, seconds
V	instantaneous resultant velocity of model, feet per second
$\dot{w}$	instantaneous velocity of peak-pressure point, feet per second $(\dot{f}\sqrt{N})$
$\dot{x}$	instantaneous velocity of model parallel to undisturbed water surface, feet per second
y	instantaneous draft of model normal to undisturbed water surface, feet

$\dot{y}$ instantaneous velocity of model normal to undisturbed water surface, feet per second

$\dot{z}$ instantaneous velocity of model normal to keel (normal to surface for flat plate), feet per second ($\dot{x} \sin \tau + \dot{y} \cos \tau$)

$\ddot{z}$ instantaneous acceleration of model normal to keel (normal to surface for flat plate), feet per second per second

β angle of dead rise, radians

γ instantaneous flight-path angle relative to undisturbed water surface, degrees $\left(\tan^{-1} \frac{\dot{y}}{\dot{x}}\right)$

ϵ auxiliary variable used as parameter in equations (6), (7), and (9), radians

η transverse distance from center line of model, feet

θ effective angle of dead rise

λ distance forward of step parallel to longitudinal center line of model, beams

λ_d length of model below undisturbed water surface, beams $\left(y/\sin \tau\right)$

λ_p wetted length based on peak-pressure location (longitudinal distance from step to position of peak pressure at model center line or keel), beams

ρ mass density of water, 1.938 slugs per cubic foot

τ trim, radians

$\varphi(A)$ aspect-ratio correction

Subscripts:

c at longitudinal center line or keel

t two-dimensional

Dimensionless variables:

C_{N_p} normal-load coefficient for rectangular flat plate $\left(\frac{F_N}{\frac{1}{2}\rho\dot{f}^2 S}\right)$

N pressure ratio $\left(\frac{1}{2}\rho\dot{w}^2/\frac{1}{2}\rho\dot{f}^2\right)$

$\frac{p}{\frac{1}{2}\rho\dot{f}^2}$ pressure coefficient based on $\dot{f}$

REVIEW OF THEORY

Theoretical impact and planing relations for symmetrical water landing conditions.- References 8 and 9 show that (with certain exceptions) planing and impacting prismatic bodies having the same geometrical conditions of angle of dead rise, trim, and wetted-length-beam ratio have essentially the same shape of pressure distribution over their wetted surfaces. The magnitudes of these pressures are in planing proportional to the square of the resultant or planing velocity of the model $\dot{x}$. In impact the pressures bear the same relation to the square of the equivalent planing velocity $\dot{f}$ which is defined by the relation $\dot{f} = \dot{x} + \dot{y} \cot \tau$. Some of the deviations from this simplified analogy between impact and planing conditions are discussed in the appendix. Although these deviations should generally be investigated, they are relatively small when compared with the experimental data used in this paper. Consequently, for simplicity it is henceforth assumed herein that planing and impact conditions are adequately related by this simple analogy. With this analogy and the laws of dynamic similarity for planing surfaces (buoyancy and viscosity being neglected) the pressure distribution on a prismatic surface, whether in impact or planing, can be expressed formally by the functional relation

$$\frac{p}{\frac{1}{2}\rho\dot{f}^2} = f_1\left(\frac{\eta}{b}, \frac{\lambda}{\lambda_p}, \lambda_p, \tau, \beta\right) \tag{1}$$

where the various geometrical parameters in this equation are illustrated in figure 1.

Longitudinal pressure distribution on an infinitely wide flat plate during steady planing.- Wagner has presented a theoretical solution for the two-dimensional flow for a semi-infinite flat plate during steady

planing on a perfect nonbuoyant fluid (fig. 2) in references 1 and 2. A more detailed analysis of this same problem is given by Pierson and Leshnover in reference 3, which presents equations that permit calculation of the longitudinal pressure distribution and the normal-load coefficient $\left(C_{N_p}\right)_t$ (or average pressure), where $\left(C_{N_p}\right)_t$ is defined by the relation

$$\left(C_{N_p}\right)_t = \frac{1}{\frac{1}{2}\rho \dot{f}^2 \lambda_p} \int_0^\infty p \, d\lambda \tag{2}$$

The theoretical pressure distribution can be expressed in the alternate forms

$$\frac{p}{\frac{1}{2}\rho \dot{f}^2} = f_2\left(\frac{\lambda}{\lambda_p}, \tau\right) \tag{3}$$

or

$$\frac{p}{\frac{1}{2}\rho \dot{f}^2} = f_3\left[\frac{\lambda}{\lambda_p}, \left(C_{N_p}\right)_t\right] \tag{4}$$

where, for two-dimensional flow, the relation between the trim and the normal-load coefficient can be expressed as

$$\left(C_{N_p}\right)_t = \frac{2\pi}{\cot \frac{\tau}{2} \cos \tau + \tan \frac{\tau}{2} \log_e\left(\frac{2}{1 - \cos \tau}\right) + \pi - \tau - \sin \tau} \tag{5}$$

Equation (5) is shown in figure 3, and calculated pressure distributions for various trims and corresponding normal-load coefficients are shown in figure 4.

Transverse pressure distribution on chine-immersed sections of flat and V-bottom surfaces for infinitely large wetted lengths.- Korvin-Kroukovsky and Chabrow have presented in reference 4 (see also reference 10) a derivation for the two-dimensional flow and pressure distribution for a symmetrical wedge (including the flat plate) completely submerged in a fluid, moving normal to the stream, and having steady separated flow behind the wedge (fig. 5). The equations presented in reference 4 for the transverse pressure distribution can be written as follows:

$$\frac{p}{p_c} = 1 - \left(\frac{\cos \epsilon}{1 + \sin \epsilon}\right)^{2h} \tag{6}$$

where p_c is the pressure at the center of the wedge and ϵ is related to the transverse distance η by the relation

$$\eta = 2kb \cos \beta \int_{\epsilon}^{\pi/2} (1 + \sin \epsilon)^h (\cos \epsilon)^{1-h} \sin \epsilon \, d\epsilon \qquad (7)$$

in which

$$\frac{1}{k} = 4 \cos \beta \int_{0}^{\pi/2} (1 + \sin \epsilon)^h (\cos \epsilon)^{1-h} \sin \epsilon \, d\epsilon$$

and

$$h = \frac{\pi - 2\beta}{\pi}$$

The average pressure is given by the following table, taken from page 105 of reference 10:

β (deg)	$\bar{p}/p_c$
0	0.879
10	.844
20	.800
30	.745
40	.677
50	.593

In reference 4 the value of p_c was given as $\frac{1}{2}\rho\dot{z}^2$ where $\dot{z}$ is the normal velocity of the wedge. Expressed in terms of the equivalent planing velocity, p_c would be given by the relation

$$\frac{p_c}{\frac{1}{2}\rho\dot{f}^2} = \sin^2\tau \qquad (8)$$

since $\dot{z} = \dot{f} \sin \tau$ (see fig. 1).

For the special case of the rectangular flat plate ($h = 1$), equation (7) reduces to

$$\eta = \frac{b}{8 + 2\pi} (\pi - 2\epsilon + 4 \cos \epsilon + \sin 2\epsilon) \qquad (9)$$

and the average pressure is

$$\frac{\overline{p}}{p_c} = 0.88 \tag{10}$$

Transverse pressure distribution on non-chine-immersed sections of V-bottom surfaces.- Wagner (references 1 and 5) has presented a derivation for the pressure distribution during the zero-trim constant-velocity impact of a wedge on a smooth water surface (fig. 6); this derivation has been modified by Pierson and Leshnover (references 6 and 7) to apply to the case of a wedge at a finite angle of trim. The equations obtained for the pressure distribution can be expressed as follows:

$$\frac{p}{\frac{1}{2}\rho \dot{f}^2} = \left[\frac{\pi \cot \theta}{\sqrt{1 - \left(\frac{\eta}{c}\right)^2}} - \frac{1}{\left(\frac{c}{\eta}\right)^2 - 1}\right] \sin^2 \tau \tag{11}$$

where

$$\tan \theta = \frac{\pi}{2} \sqrt{\frac{\sin^2 \beta + K^2 \tan^2 \tau}{K^2 - 2K \sin^2 \beta - K^2 \sin^2 \beta \tan^2 \tau}}$$

and

$$K \approx \frac{\pi}{2}\left(1 - \frac{3 \tan^2 \beta \cos \beta}{1.7\pi^2} - \frac{\tan \beta \sin^2 \beta}{3.3\pi}\right)$$

ANALYSIS AND DISCUSSION

Pressure Distribution on a Rectangular Flat Plate of Finite Length-Beam Ratio

General observations.- Observations of the experimental pressure distributions of reference 9 (see for example fig. 7) indicate that for a given pressure distribution the pressures along the longitudinal center line of a flat plate are larger than the corresponding pressures along all other longitudinal sections and that the pressure distributions in other longitudinal sections are similar in shape to the center-line distributions but decrease in magnitude toward the edge of the plate. In other words, for the flat plate, equation (1) can be expressed more simply as

$$\frac{p}{\frac{1}{2}\rho \dot{f}^2} = \frac{p_c}{\frac{1}{2}\rho \dot{f}^2} \frac{p}{p_c} \tag{12}$$

where

$$\frac{p_c}{\frac{1}{2}\rho \dot{f}^2} = f_4\left(\frac{\lambda}{\lambda_p}, \lambda_p, \tau\right) \tag{13}$$

$$\frac{p}{p_c} = f_5\left(\frac{\eta}{b}\right) \tag{14}$$

and $f_5\left(\frac{\eta}{b}\right)$ is unity at the center line and decreases to zero at the sides of the plate.

Transverse pressure distribution.- The theoretical transverse distribution of pressure on a flat plate is known for the two limiting cases of very small (infinitesimal) and very large (infinite) wetted lengths. For very small wetted lengths $(\lambda_p \rightarrow 0)$ the transverse pressure distribution obviously is

$$\frac{p}{p_c} = 1 \qquad (\lambda_p \rightarrow 0) \tag{15}$$

and for very large wetted lengths $(\lambda_p \rightarrow \infty)$ the transverse pressure distribution is given by equations (6) and (9). These two theoretical pressure distributions are shown in figure 8 together with some experimental data from reference 9. The experimental data appear, on the average, to lie somewhere between the two theoretical limiting conditions. The average value of the experimental pressure $\overline{p}/p_c$ is approximately

$$\frac{\overline{p}}{p_c} = 0.95 \tag{16}$$

Longitudinal distribution of pressure at model center line.- From a comparison of the experimental data with the theory for the longitudinal pressure distribution on the two-dimensional flat plate (compare figs. 4 and 7), the shape of the experimental curves is found to be similar to the shape of the theoretical curves, but the curves are not quantitatively similar for the same experimental and theoretical trims. However, the experimental and theoretical pressure distributions along the center line are usually found to be quantitatively similar for the same

experimental and theoretical normal-load coefficients (see equation (4) with c replacing t to denote center-line conditions). The experimental longitudinal center-line pressure may thus be expressed formally as

$$\frac{p_c}{\frac{1}{2}\rho f^2} = f_3\left[\frac{\lambda}{\lambda_p}, \left(C_{N_p}\right)_c\right] \tag{17}$$

where $f_3\left[\frac{\lambda}{\lambda_p}, \left(C_{N_p}\right)_c\right]$ is the theoretical pressure distribution given in figure 4 in which the subscript t is replaced by c to denote the normal-load coefficient of the center-line strip.

In order to use equation (17), the variation of $\left(C_{N_p}\right)_c$ with trim and wetted length must be known. This knowledge is not generally available but experimental data are available that are suitable for determining the variation of the average normal-load coefficient C_{N_p} with trim and wetted length. These two normal-force coefficients may be related by means of the average transverse pressure distribution by the relation

$$\left(C_{N_p}\right)_c = \frac{C_{N_p}}{\overline{p}/p_c} \tag{18}$$

An example of the variation of C_{N_p} with trim and wetted length is shown in figure 9 which is a cross plot of Locke's high-speed planing data from reference 11 drawn to the theoretical end point for $\lambda_p \longrightarrow 0$ given by equation (5).

In order to determine the accuracy of equation (17), experimental longitudinal center-line pressure distributions from reference 9 are compared in figure 10 with pressure distributions computed from equations (17) and (18) by using the two limiting values of $\overline{p}/p_c$ according to equations (10) and (15). The values of C_{N_p} needed for these computations were taken from figure 9 for the cases which fell within the range of the curves shown, and for other cases C_{N_p} was computed from the impact data of reference 9. From these values $\left(C_{N_p}\right)_c$ was determined from equation (18). The experimental pressures for the trims of 30° and lower for all wetted lengths tested are seen to be in rather good agreement with the computed values, the data generally falling somewhere between the two limit curves for $\frac{\overline{p}}{p_c} = 1$ and $\frac{\overline{p}}{p_c} = 0.88$; thus

a value of $\frac{\overline{p}}{p_c}$ equal to approximately 0.95 would probably give the best over-all agreement.

Proposed method.- The preceding discussion can be summarized into a semiempirical proposed method for computing the pressure distribution on a rectangular flat plate during impact or planing as indicated by the following steps:

(1) The average normal-load coefficient C_{N_p} is obtained from figure 9 or from any other available source.

(2) The center-line normal-force coefficient $\left(C_{N_p}\right)_c$ is computed from the relation

$$\left(C_{N_p}\right)_c = \frac{C_{N_p}}{0.95} \tag{19}$$

given by equations (16) and (18).

(3) The pressure distribution along the longitudinal center line is computed from the relation

$$\frac{p_c}{\frac{1}{2}\rho \dot{r}^2} = f_3\left[\frac{\lambda}{\lambda_p}, \left(C_{N_p}\right)_c\right]$$

where, by substituting the subscript c for t, this relation is given by figure 4.

(4) The transverse pressure distribution is computed as the average between the value predicted by equations (6) and (9) and the value predicted by equation (15).

Limitations of method.- Although the foregoing procedure provides a reasonable estimate of the pressure distribution for most of the conditions of trim and wetted length encountered during the tests of reference 9 ($\tau < 30^\circ$; $\lambda_p < 3.3$), it may not be so satisfactory for much larger wetted lengths. For such cases it is more likely that the flow in regions remote from the leading or trailing edges of the plate can be considered to occur primarily in two-dimensional planes stationary in space and oriented normal to the model longitudinal center line. Then according to reference 4 the magnitude of the center-line pressure will be uniform and equal to $\frac{1}{2}\rho \dot{z}^2$ where $\dot{z}$ is the velocity of

the model normal to its surface which is related to the equivalent planing velocity by the relation $\dot{z} = \dot{f} \sin \tau$ (see fig. 1) so that the predicted center-line pressure coefficient is $\frac{p_c}{\frac{1}{2}\rho \dot{f}^2} = \sin^2 \tau$ (equation (8)).

The longitudinal distribution of pressure, according to this limiting condition, should be uniform except near the leading and trailing edges. (In the very small region of the trailing edge the pressure will drop to zero and in the very small region of the leading edge ($\lambda = \lambda_p$), it will rise to equal the dynamic pressure $\frac{1}{2}\rho \dot{f}^2$.) However, an examination of figure 9 shows that the experimental data do not tend to obey equation (8) or to approach a uniform longitudinal distribution of pressure. The proposed procedure for computing the flat-plate pressures may therefore give reasonable results for wetted lengths greater than those tested ($\lambda_p < 3.3$). However, for extremely large wetted lengths the procedure will fail. For such cases the center-line normal-load coefficient is, from equation (8), equal to

$$\left(C_{N_p}\right)_c = \frac{p_c}{\frac{1}{2}\rho \dot{f}^2} = \sin^2 \tau$$

For example, for an infinitely long flat plate at a trim of 30°, $\left(C_{N_p}\right)_c = 0.25$. Because the pressure distribution for $\left(C_{N_p}\right)_c = 0.25$ in figure 4 is far from the theoretically required uniform distribution, it is evident that the procedure fails for this limiting case.

Pressure Distribution on a V-Bottom Prismatic Surface

For the treatment of a V-bottom prismatic surface, it is convenient to separate the wetted surface into two regions of concern (see fig. 1); namely, (1) the region forward of the intersection of the water surface with the chines and (2) the region aft of this intersection.

Transverse pressure distribution.- For non-chine-immersed sections, Pierson and Leshnover have proposed equation (11) for the transverse pressure distribution on V-bottom planing surfaces. (Some information regarding step losses is also given in reference 7.) Comparisons with experimental data for angles of dead rise of 20° and 30° given in references 6 and 8, respectively, indicate that the predictions of these equations are reasonable for trims below approximately 15° but that they may be unconservative for larger angles of trim. For such cases (large trims) some more accurate information is given by the peak-pressure analysis of reference 8.

For chine-immersed sections of V-bottom surfaces it has been indicated in reference 8 that the transverse shape of the pressure distribution on a surface having an angle of dead rise of 30° is qualitatively but not quantitatively similar to the predictions of reference 4 (equations (6) to (8)); that is, equations (6) and (7) are in reasonable agreement with the experimental data but equation (8) is not.

Longitudinal pressure distribution.- In the region where the chines are immersed below the water surface, some similarity exists between the longitudinal pressure distributions on flat and dead-rise surfaces (compare figs. 7 and 11). Specifically, figure 12 shows that the pressure distribution along the longitudinal center line of the flat plate ($\beta = 0^\circ$) is approximately the same as that on a model having an angle of dead rise of 30° for the same trim and wetted length over the chine-immersed part of the V-bottom surface. The agreement is seen to be best where the chine-immersed fraction of the total wetted area (see vertical arrows in fig. 12) is large. Where this fraction is small, as in the first two parts of figure 12, the agreement is not so good.

Proposed procedure.- The preceding observations suggest that the following procedure may give, in general, a reasonable prediction of the pressure distribution on V-bottom surfaces for angles of dead rise at least up to 30°. It is assumed that the instantaneous velocities, the trim, the angle of dead rise, and the wetted length are known. First, compute the longitudinal distribution of pressure along the center line of a flat plate having the same trim and wetted length and use this result for the longitudinal center-line distribution on the chine-immersed sections of the V-bottom surface. The transverse distribution of pressure is computed from equation (11) for non-chine-immersed sections and from equations (6) and (7) for chine-immersed sections.

CONCLUDING REMARKS

A semiempirical procedure has been presented for predicting the water-pressure distribution on rectangular flat plates and V-bottom prismatic surfaces during impact or planing. According to this procedure, for the case of the rectangular flat plate the longitudinal center-line distribution of pressure is a function only of the normal-load coefficient, which function can be predicted from the theory for the two-dimensional problem given by Wagner. The transverse distribution of pressure is obtained as a compromise between the available theoretical treatments for very small and very large wetted-length-beam ratios. Comparisons with experimental data indicate that the proposed theory may give reasonable predictions of the pressure distribution for most practical conditions.

For the case of the V-bottom surface of finite angle of dead rise, the analysis assumes that the longitudinal center-line distribution of pressure on chine-immersed sections of a V-bottom prismatic surface is

the same as that on the corresponding flat plate and that the transverse distribution of pressure on non-chine-immersed and chine-immersed sections is given by the theories of Wagner and Pierson and of Korvin-Kroukovsky and Chabrow, respectively. Although experimental data for an angle of dead rise of 30° indicate that the proposed procedure may work fairly well for this case, the available data are not sufficient for determining the general value of the procedure for V-bottom surfaces.

Langley Aeronautical Laboratory
National Advisory Committee for Aeronautics
Langley Field, Va., October 1, 1951

APPENDIX

DEVIATIONS FROM SIMPLE IMPACT-PLANING RELATION

Effect of wave rise on a rectangular flat plate.- In the case of a short flat surface ($\lambda_p < 1.5$) the relations between impacting and planing surfaces are complicated by the presence of a forward splash-up of water in front of the plate; see the following sketch:

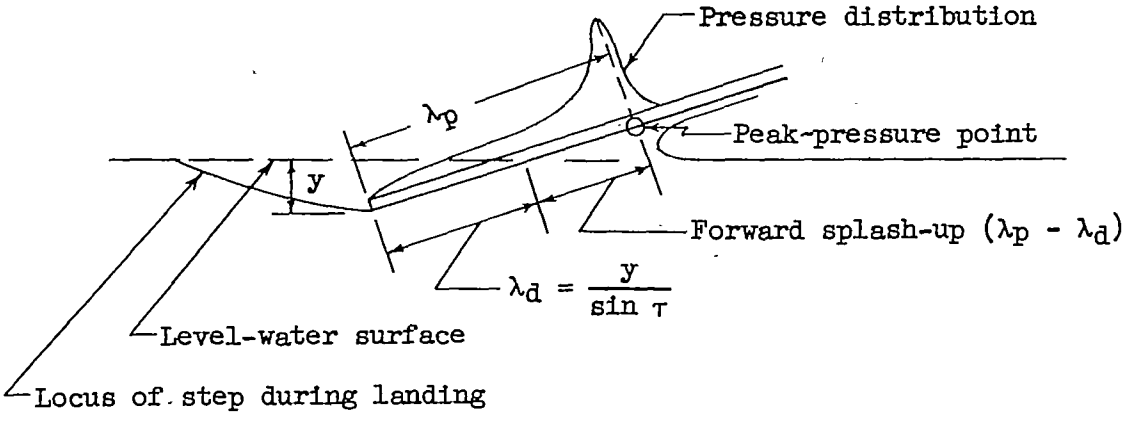

The rate of change of this splash-up during an impact causes an additional increment of force on the plate. As a first approximation this effect is the same as if the equivalent planing velocity were replaced by a more general velocity $\dot{w}$, the velocity of the peak-pressure point (see reference 9), the ratio between $\dot{w}$ and f being given approximately in reference 9 as

$$N = \frac{\frac{1}{2}\rho \dot{w}^2}{\frac{1}{2}\rho \dot{f}^2} = 1 + 2 \cos \tau \frac{\sin \gamma}{\sin(\gamma + \tau)}\left(\frac{d\lambda_p}{d\lambda_d} - 1\right) + \left[\frac{\sin \gamma}{\sin(\gamma + \tau)}\left(\frac{d\lambda_p}{d\lambda_d} - 1\right)\right]^2 \tag{A1}$$

that is, the pressures predicted by the equations proposed in the body of the paper should be multiplied by the ratio N. For large wetted-length-beam ratios, the splash-up is constant $\left(\frac{d\lambda_p}{d\lambda_d} - 1 = 0\right)$ and $N = 1$; for small flight-path angles ($\gamma \to 0$), N also reduces to unity. For small wetted-length-beam ratios $(\lambda_p < 1.5)$ at high flight-path angles, however, the ratio may be considerably greater than unity.

Effect of deceleration normal to the keel.- During a landing a component of model deceleration exists normal to the keel (normal to the surface for the flat plate) and results in a slight distortion of the pressure distribution on an impacting body from that on a planing body. As a first approximation for this effect the derivation of Wagner (reference 1) gives the pressure due to acceleration (which is usually negative) as

$$p = \rho \ddot{z} c \sqrt{1 - \left(\frac{\eta}{c}\right)^2} \tag{A2}$$

where c is the wetted semiwidth of the model in any transverse plane. Equation (A2) was derived by assuming two-dimensional flow in transverse flow planes. Since this assumption is only reasonable for large wetted lengths, it is recommended that equation (A2) be corrected by an aspect-ratio correction $\varphi(A)$ so that

$$p = \rho \ddot{z} c \varphi(A) \sqrt{1 - \left(\frac{\eta}{c}\right)^2} \tag{A3}$$

The hydrodynamic aspect ratio is defined as

$$A = \frac{\lambda_p^2}{S} \tag{A4}$$

and the suggested aspect-ratio correction is

$$\varphi(A) = \sqrt{\frac{1}{1 + \frac{1}{A^2}}}\left(1 - \frac{0.425}{A + .\frac{1}{A}}\right) \qquad (0 < A < \infty) \tag{A5}$$

or

$$\varphi(A) = 1 - \frac{1}{2A} \qquad (A > 1.5) \tag{A6}$$

(Equations (A5) and (A6) were obtained by Pabst (references 12 and 13) from vibration tests of rectangular flat plates.) When the pressure computed from equation (A3) is large compared with the pressures predicted in the body of the paper, it should be added to those pressures.

REFERENCES

1. Wagner, Herbert: Über Stross- und Gleitvorgänge an der Oberfläche von Flüssigkeiten. Z.f.a.M.M., Bd. 12, Heft 4, Aug. 1932, pp. 193-215.

2. Wagner, Herbert: Planing of Watercraft. NACA TM 1139, 1948.

3. Pierson, John D., and Leshnover, Samuel: An Analysis of the Fluid Flow in the Spray Root and Wake Regions of Flat Planing Surfaces. Preprint No. 166, S.M.F. Fund Paper, Inst. Aero. Sci. (Rep. No. 335, Project No. NR 062-012, Office of Naval Res., Exp. Towing Tank, Stevens Inst. Tech.), Oct. 1948.

4. Korvin-Kroukovsky, B. V., and Chabrow, Faye R.: The Discontinuous Fluid Flow past an Immersed Wedge. Preprint No. 169, S.M.F. Fund Paper, Inst. Aero. Sci. (Rep. No. 334, Project No. NR 062-012, Office of Naval Res., Exp. Towing Tank, Stevens Inst. Tech.), Oct. 1948.

5. Wagner, Herbert: Landing of Seaplanes. NACA TM 622, 1931.

6. Pierson, John D.: On the Pressure Distribution for a Wedge Penetrating a Fluid Surface. Preprint No. 167, S.M.F. Fund Paper, Inst. Aero. Sci. (Rep. No. 336, Project No. NR 062-012, Office of Naval Res., Exp. Towing Tank, Stevens Inst. Tech.), June 1948.

7. Pierson, John D., and Leshnover, Samuel: A Study of the Flow, Pressures, and Loads Pertaining to Prismatic Vee-Planing Surfaces. S.M.F. Fund Paper No. FF-2, Inst. Aero. Sci. (Rep. No. 382, Project No. NR 062-012, Office of Naval Res., Exp. Towing Tank, Stevens Inst. Tech.), May 1950.

8. Smiley, Robert F.: A Study of Water Pressure Distributions during Landings with Special Reference to a Prismatic Model Having a Heavy Beam Loading and a 30° Angle of Dead Rise. NACA TN 2111, 1950.

9. Smiley, Robert F.: An Experimental Study of Water-Pressure Distributions during Landings and Planing of a Heavily Loaded Rectangular Flat-Plate Model. NACA TN 2453, 1951.

10. Lamb, Horace: Hydrodynamics. Sixth ed., Cambridge Univ. Press, 1932, pp. 94-105.

11. Locke, F. W. S., Jr.: Tests of a Flat Bottom Planing Surface to Determine the Inception of Planing. NAVAER DR Rep. 1096, Bur. Aero., Dec. 1948.

12. Pabst, Wilhelm: Theory of the Landing Impact of Seaplanes. NACA TM 580, 1930.

13. Pabst, Wilhelm: Landing Impact of Seaplanes. NACA TM 624, 1931.

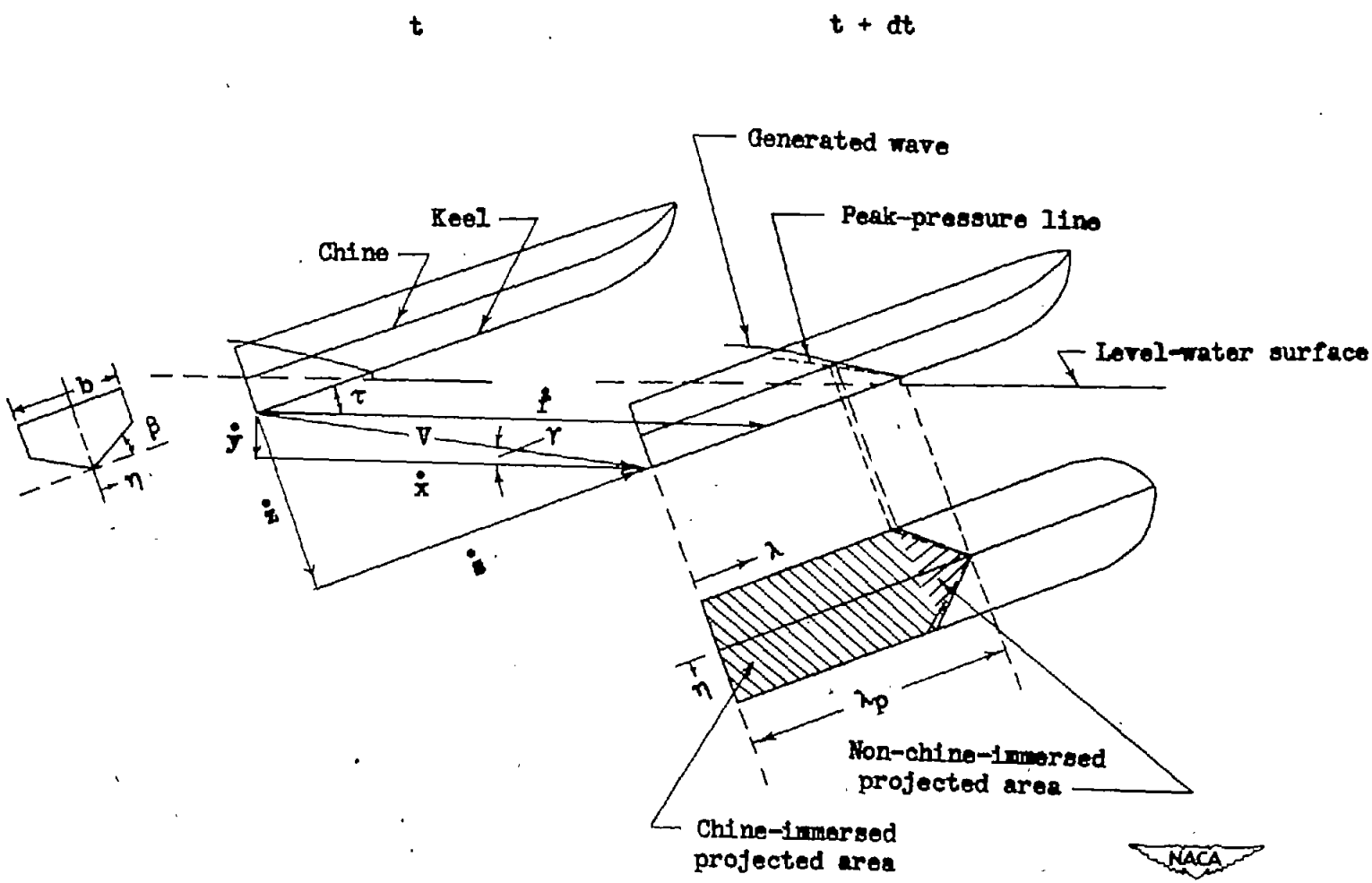

Figure 1.- Geometric relations during a landing.

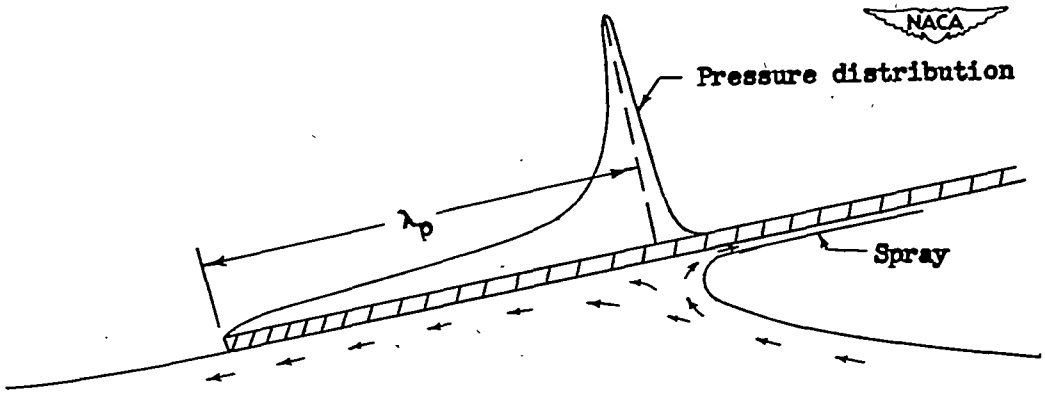

Figure 2.- The two-dimensional flow about a planing flat plate. Longitudinal section of plate.

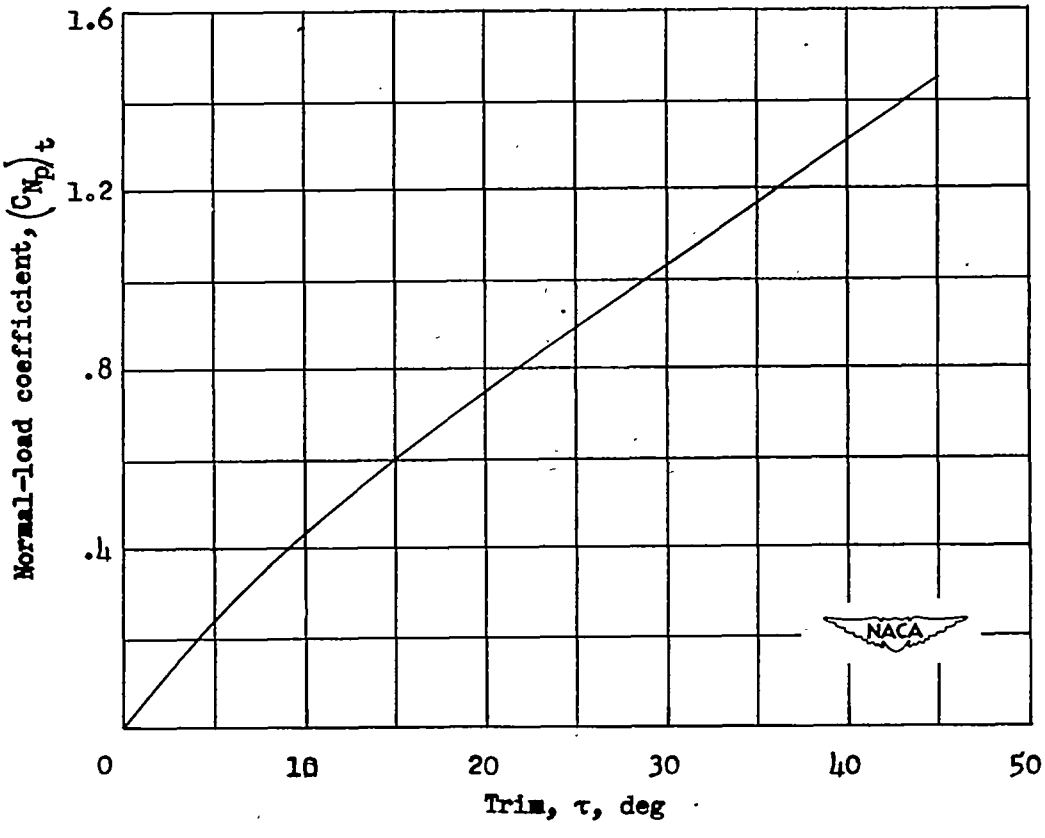

Figure 3.- Theoretical two-dimensional normal-load coefficient calculated from reference 3.

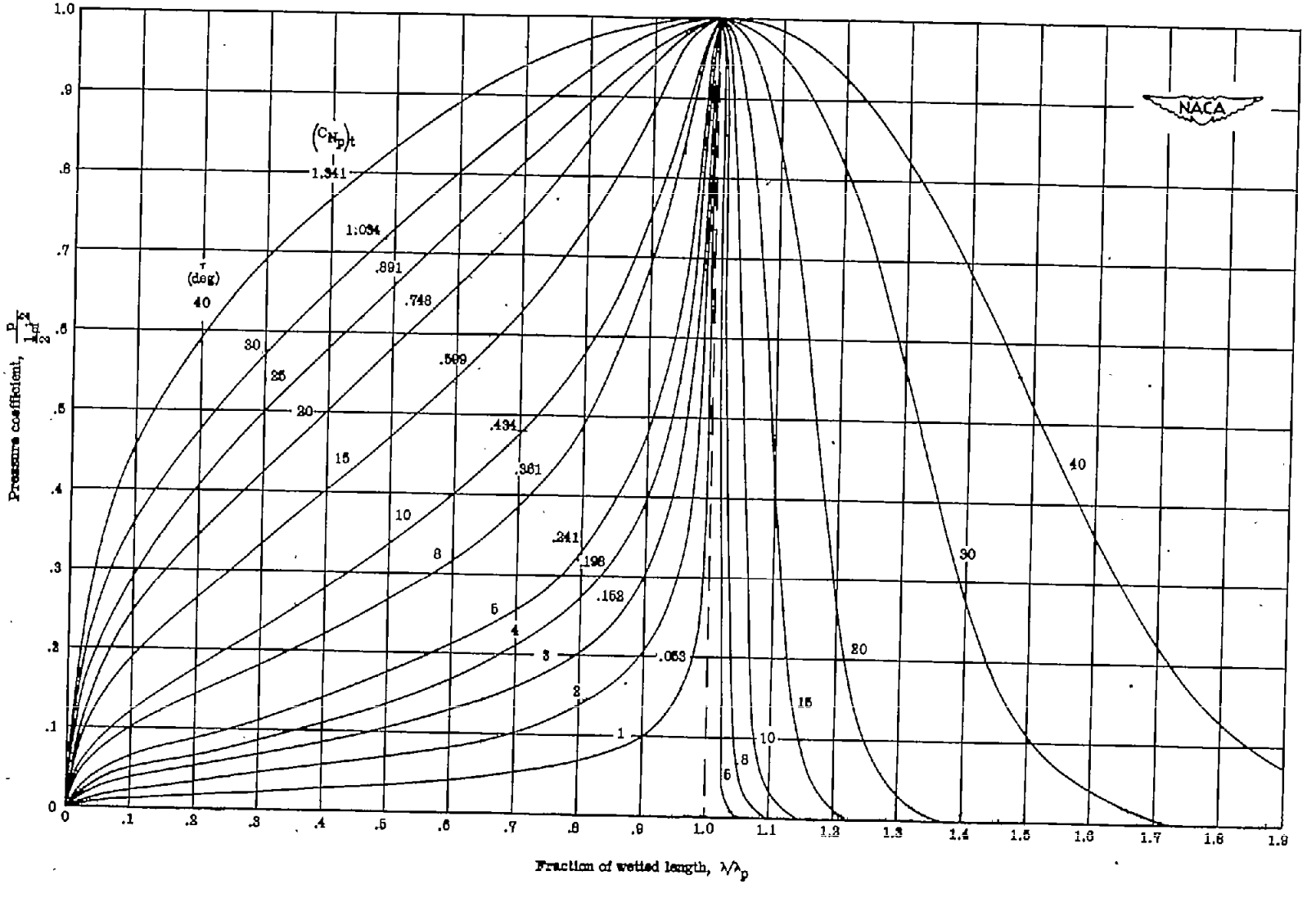

Figure 4.- Theoretical pressure distributions for the two-dimensional flat plate during steady planing calculated from reference 3.

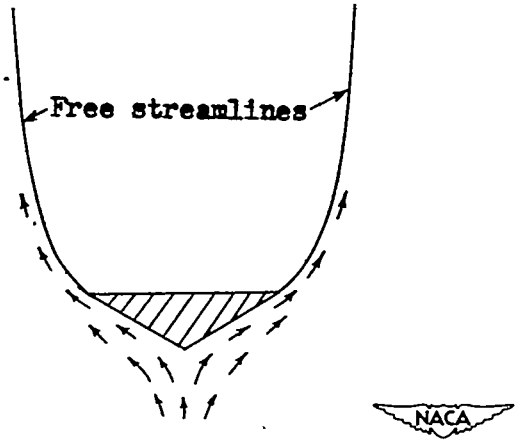

Figure 5.- The two-dimensional separated flow about a submerged wedge. Transverse section of wedge.

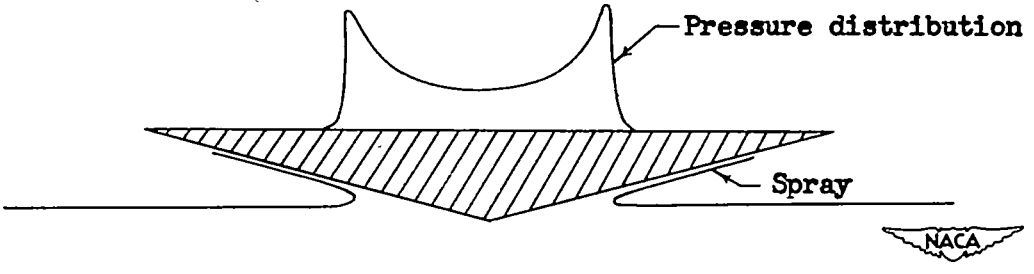

Figure 6.- The two-dimensional flow for the impact of a wedge on a smooth water surface. Transverse section of wedge.

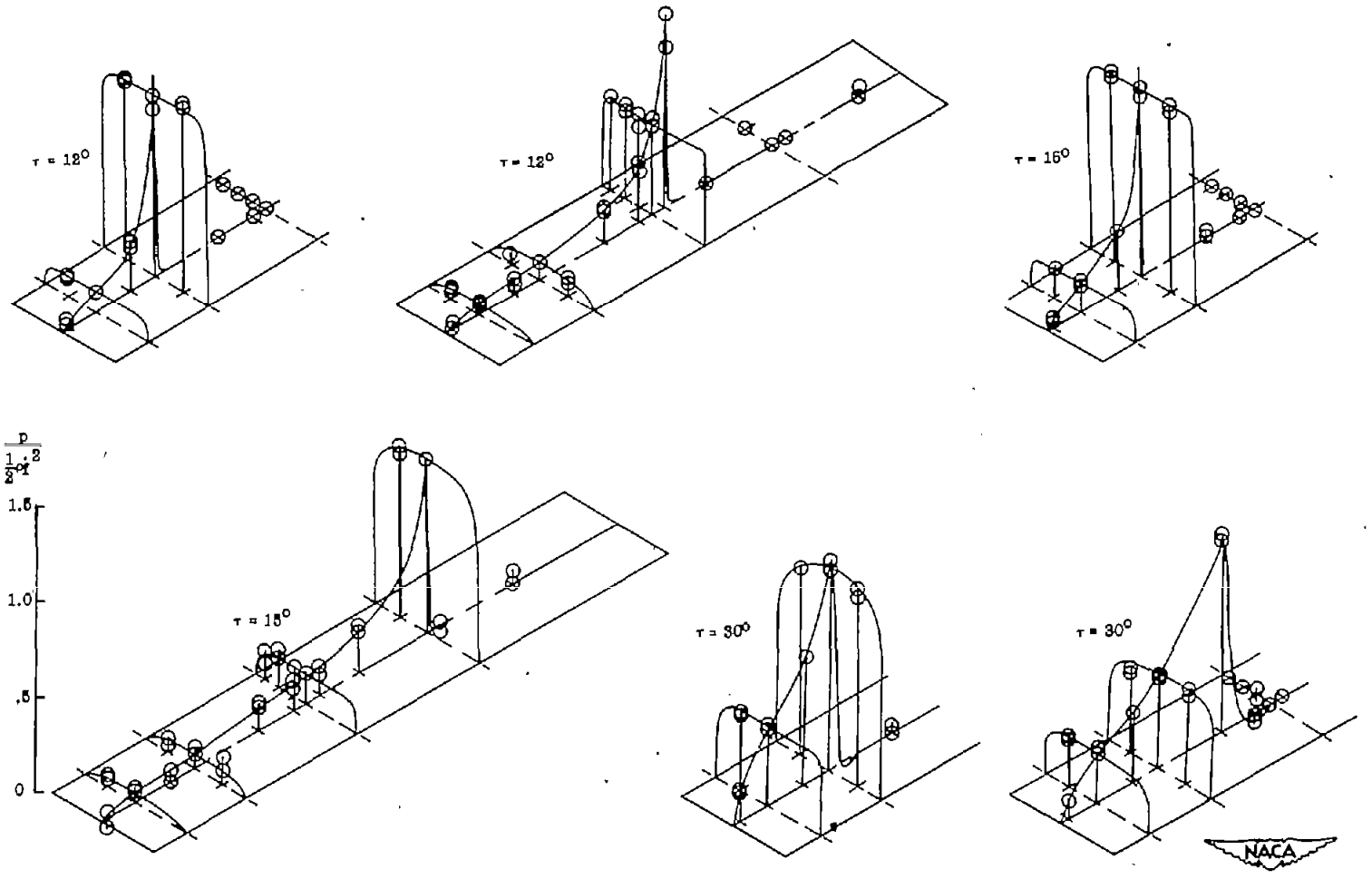

Figure 7.- The experimental distribution of pressure on a rectangular flat plate. (Experimental data from reference 9.)

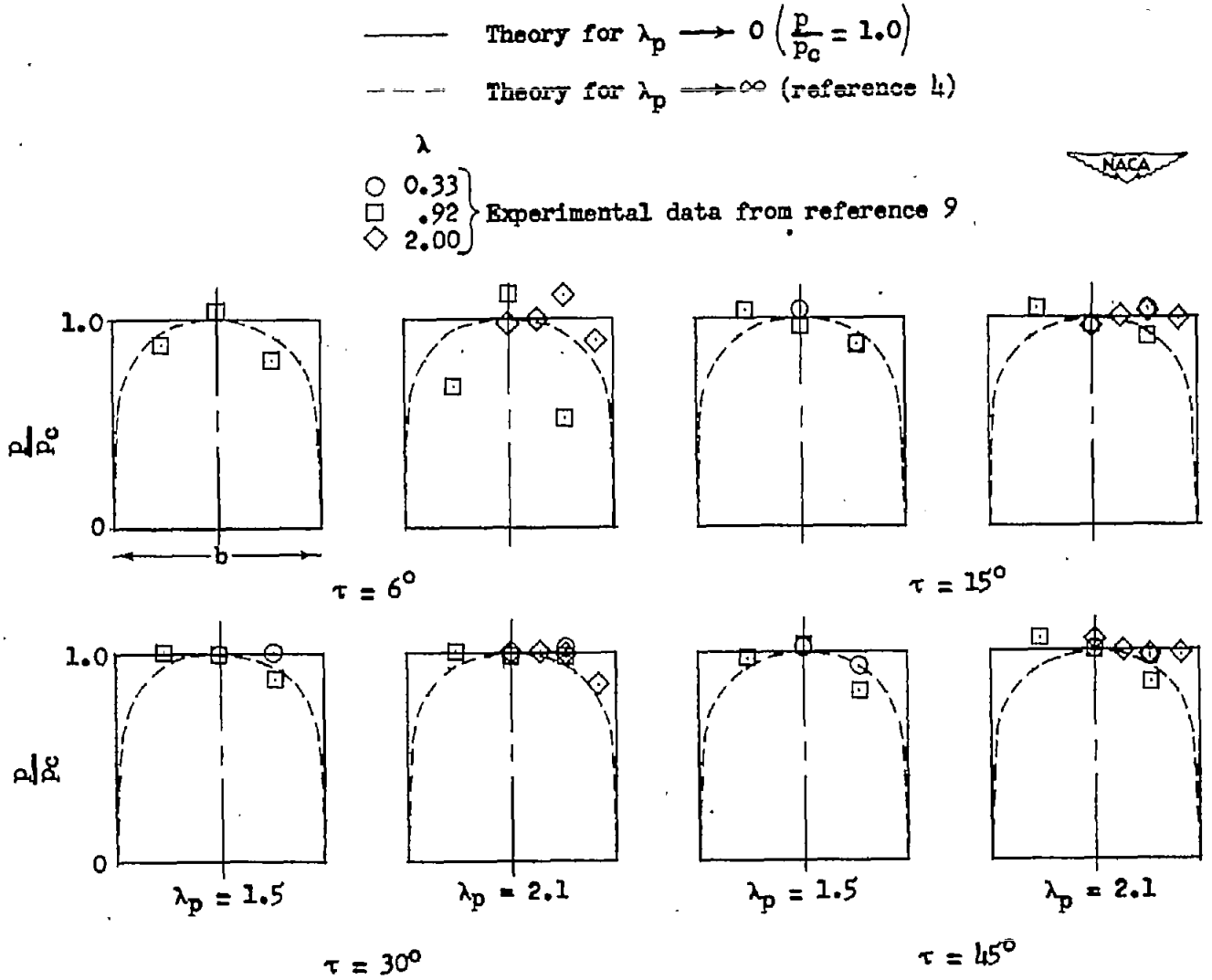

Figure 8.- The transverse distribution of pressure on a rectangular flat plate.

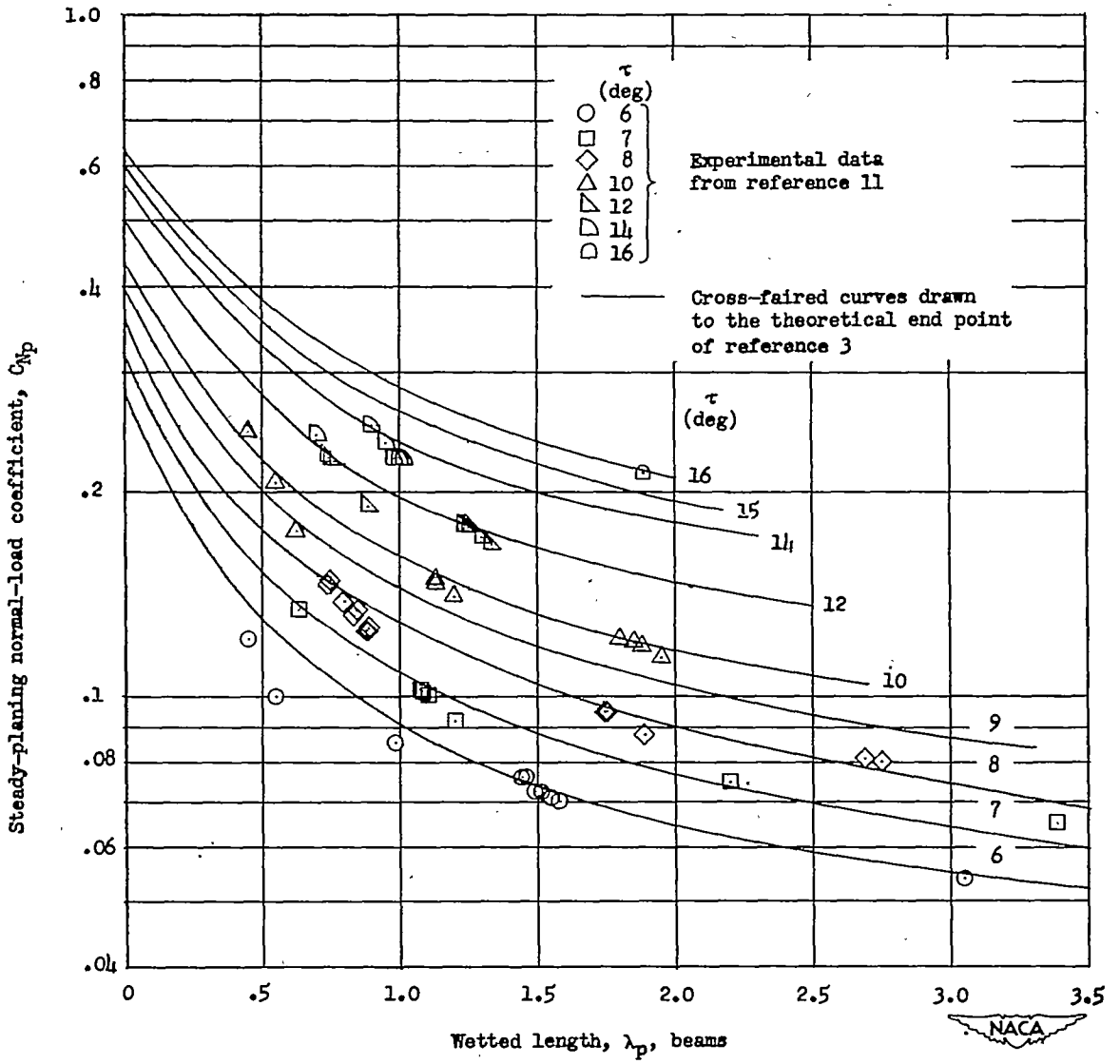

Figure 9.- High-speed steady-planing normal-load coefficients.

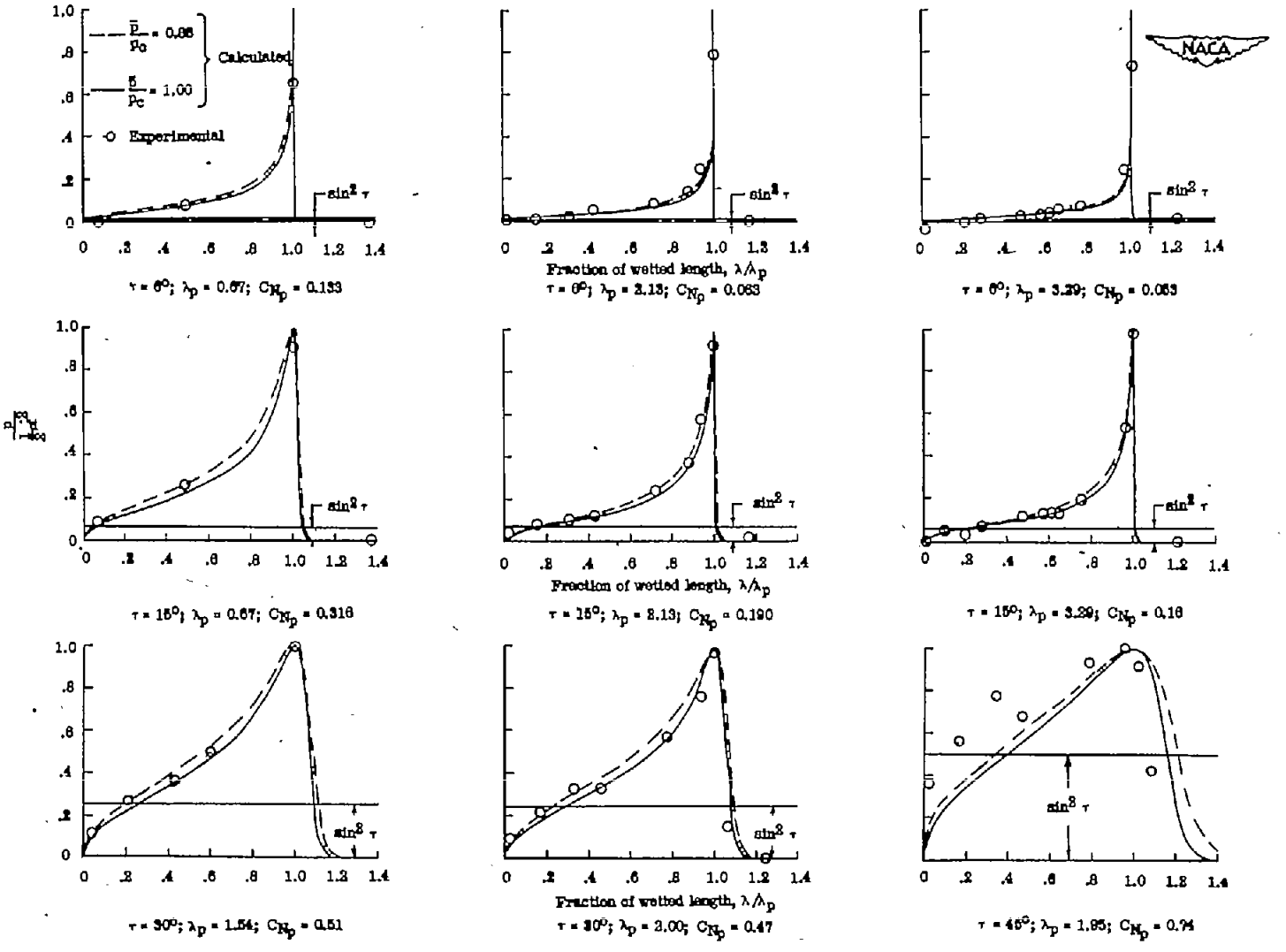

Figure 10.- The longitudinal distribution of pressure on a rectangular flat plate at the center line of the model.

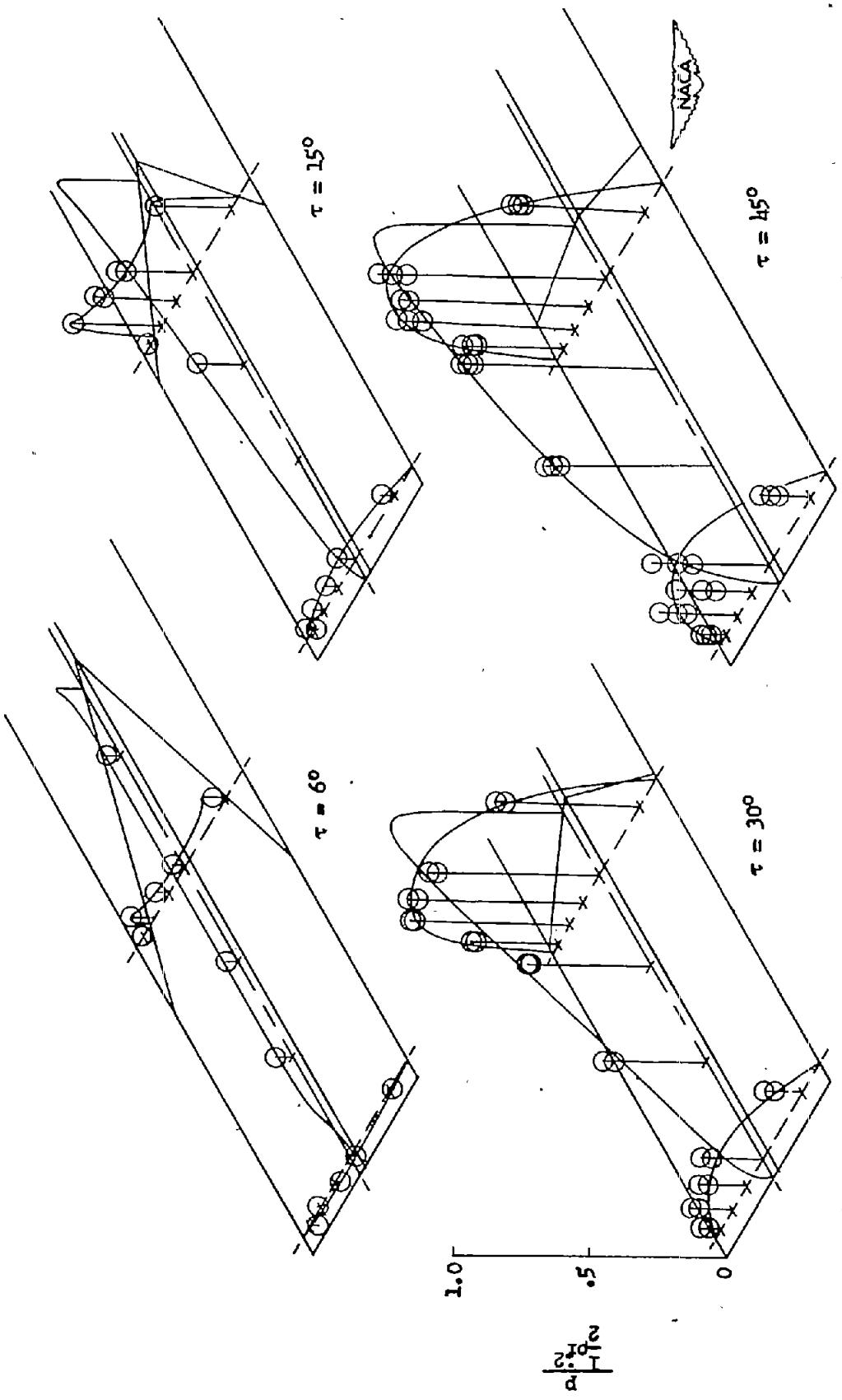

Figure 11.- The experimental distribution of pressure on a prismatic surface having an angle of dead rise of 30°. (Experimental data from reference 8.)

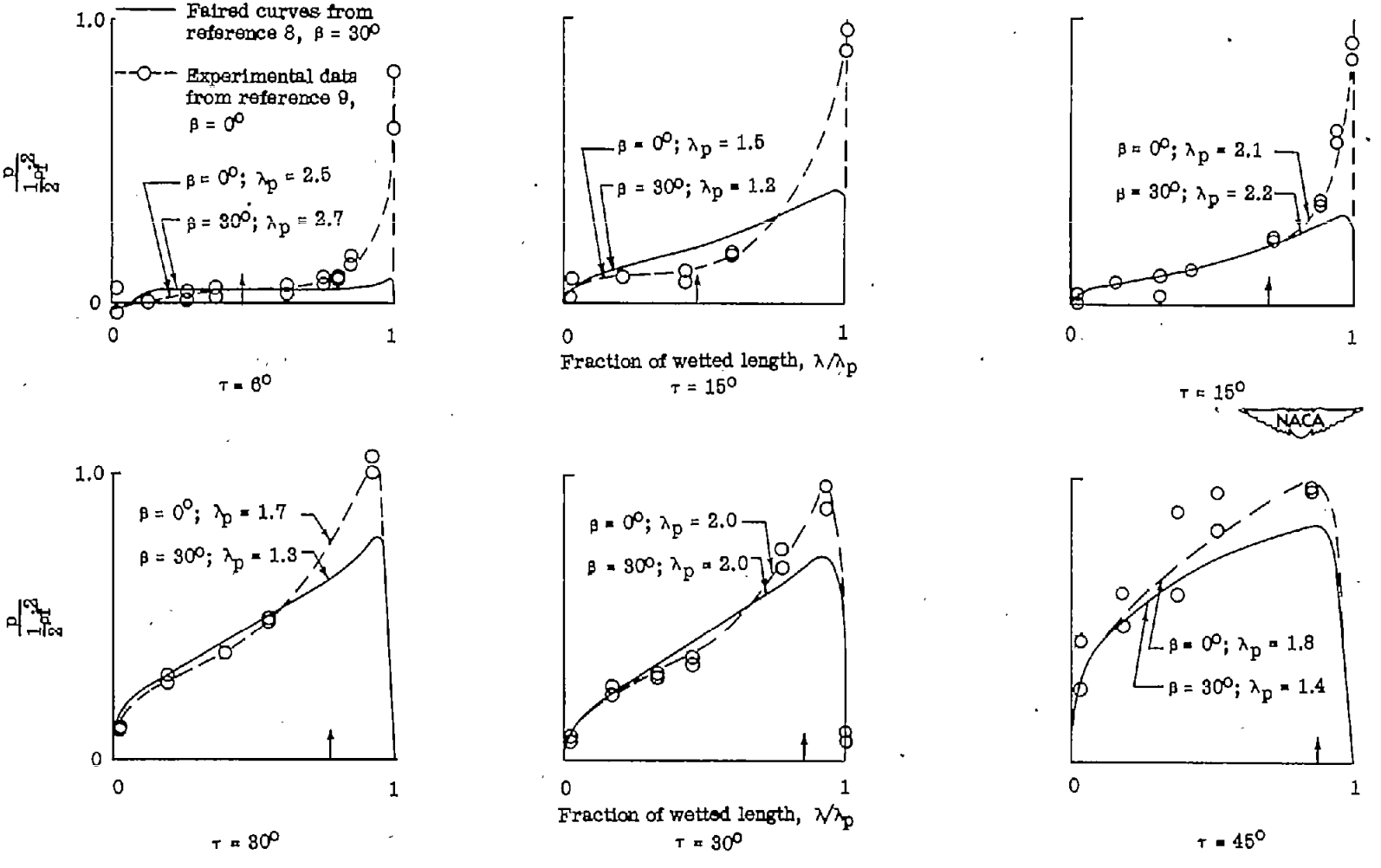

Figure 12.- Comparison of longitudinal-pressure-distribution coefficients at the keel for similar models having angles of dead rise of 0° and 30°. (Vertical arrows indicate the longitudinal position where the chines of the 30° model become immersed.)

NACA-Langley - 12-18-51 - 1000